Available online at www.sciencedirect.com
ScienceDirect
Trans. Nonferrous Met. Soc. China 25(2015) 1605−1613
Transactions of Nonferrous Metals Society of China
www.tnmsc.cn

An upper bound analysis of rolling process of non-bonded sandwich sheets

Heshmatollah HAGHIGHAT, Pedram SAADATI

Mechanical Engineering Department, Razi University, Kermanshah, Iran

Received 4 August 2014; accepted 17 December 2014

Abstract: Rolling process of symmetrical non-bonded sandwich sheets was investigated by the method of upper bound. A deformation model was proposed and the mathematical relations of the velocity components were developed. The internal, shear and frictional power terms were derived and used in the upper bound model. Through the analysis, the rolling force, mean contact pressure and final thickness of each layer were determined. The validity of the proposed analytical model was discussed by comparing the theoretical predictions with the experimental data found in the literatures. Effects of various rolling conditions such as the flow stress ratio, initial thickness ratio of the raw sheets and total thickness reduction upon the rolling torque were analyzed. The accuracy of the developed analytical model was very high.

Key words: flat rolling; sandwich sheet; upper bound method

1 Introduction

Multilayer sheets, consisting of two or more different material layers, make it possible to combine properties of dissimilar sheet metals. For example, one metal may be used for its strength and another for its ability to conduct heat, or to offer greater resistance to wear or corrosion. Multilayered sheet metal products are used in a variety of industries, such as fabrication of containers, pressure vessels and atomic energy applications. One of the most widely used multilayered sheet materials are sandwich sheet materials consisting of two different kinds of sheets. Because of the contact pressure and the relative sliding between sheets in flat rolling of sandwich sheets, this process is a suitable choice for producing sandwich sheet materials [1,2]. In this process, accurate prediction of the required torque, the roll force and final thickness of each layer is a major issue.

Among various methods of solution to metal forming processes, the upper bound method as an analytical method and finite element method has been widely used in the analysis of rolling process effectively. In spite of the recent developments of the finite element method, the appeal of the upper bound method among metal forming researchers is still strong and stems from its ability to represent material behavior, helping them in understanding the existing processes and screening ideas for new developments.

In the past, a number of investigators have presented mathematical analyses for the flat rolling of sandwich sheet materials. Based on the upper bound theorem, HWANG et al [3,4] proposed theoretical models to investigate the deformation behavior of the multilayer sheets in the rolling process. A mathematical model using stream functions and the upper bound method has been proposed by the present authors to investigate the plastic deformation behavior of sheets at the roll gap with the assumption that the bonding is completed after rolling [5,6]. MALEKI et al [7] developed an analytical model based on upper bound method for flat rolling of bimetal strips. The deformation region was divided into six rigid regions and for constructing each deformation region, a large number of assumptions were made. ZHANG et al [8] proposed a three-dimensional velocity field for single layer plate rolling by global weighted method assuming that cross-sections remained plane and vertical lines remained straight. The rolling force and torque were calculated and compared with those of experimental ones. MARTINS [9] presented an approach based on a solution resulting from the combination of the upper bound method with the weighted residuals method for analysing plane strain single layer rolling. He assumed that the plastic deformation zone was bounded by two

Corresponding author: Heshmatollah HAGHIGHAT; Tel: +98-83-34274530; Fax: +98-83-34274542; E-mail: hhaghighat@razi.ac.ir
DOI: 10.1016/S1003-6326(15)63764-5

planes perpendicular to the symmetry axis and contact surface. DOGRUOGLU [10] presented a method for constructing kinematically admissible velocity fields, which were necessary in the analysis of the flat rolling process by the upper bound method. It was assumed that the trajectories followed by the material point in the plastic deformation zone could be represented as a one-parameter family of curves in Cartesian coordinates. In the analysis, he assumed that one of the entry or exit surfaces to the deformation zone was plane perpendicular to the symmetry axis.

In the current research, the kinematically admissible velocity field for the rolling of sandwich sheets, non-bonded before rolling, and discussion of some mathematical aspects involved in this method are presented in details. The internal, shear and frictional power terms are derived. The analytical rolling torque and roll separating force are compared with the experimental data in Refs. [4,6].

2 Rolling process of sandwich sheets

Figure 1 shows the rolling process of a sandwich sheet where sheet layers are not bonded before rolling. The process has one symmetry plane, and then, only half of the section is considered. An initially symmetrical sandwich sheet, made of two different ductile materials with the mean flow stresses σ_{0o} and σ_{0i}, is considered. The subscripts "o" and "i" denote outer and inner layers, respectively. The material starts as an un-bonded sandwich sheet with initial thicknesses t_{1o} and t_{2o} for outer and inner layers, respectively and it rolls into a completely bonded sandwich sheet with thickness of t_{1f} and t_{2f} for the outer and inner layers, respectively.

Through the analysis, the following assumptions are employed: 1) The roll is rigid material; 2) The sandwich sheet is symmetric on both the material and the thickness about symmetry axis; 3) The sheets are rigid plastic materials; 4) The deformation of the sheet is plane strain; 5) A constant friction factor is applied on the frictional surfaces; 6) At the exit of deformation region, a unified velocity distribution is obtained, which means that the bonding of the sheets after the rolling process is completed and there is no relative motion between the two layer materials; 7) The frictional force between the two materials before entering the deformation zone is neglected.

The general deformation model, where the outer and inner layers are rolled with different thickness ratios, is shown in Fig. 1. The material under deformation of each layer is divided into three regions. In regions I_o, I_i, III_o and III_i, the materials are rigid and move as rigid bodies. Before entering the deformation region, the two materials move at different speeds v_{1o} and v_{2o}; after rolling, the two materials move at the same velocity v_f in the axial direction.

Since it is assumed that there is no change in width and because of volume constancy, the following relation holds

$$v_{1o}t_{1o} = v_f t_{1f}, \quad v_{2o}t_{2o} = v_f t_{2f} \tag{1}$$

Regions II_o and II_i are the deformation regions. Region II_o is surrounded by two cylindrical velocity discontinuity surfaces, S_1 and S_2, and the interface surface A_3 as well as the contact surface S_3. Region II_i is bounded by two cylindrical velocity discontinuity surfaces A_1 and A_2 as well as the interface surface A_3. Two cylindrical coordinate systems with origins O_1 and O_2 are used to describe the positions of the four surfaces of velocity discontinuity, contact surface S_3, interface surface A_3, and the velocity components in deformation regions. The center of the cylindrical boundaries of the deformation region II_o, S_1 and S_2, is O_1 and they are located at distances r_{1o} and r_{1f} from the origin O_1, respectively. The mathematical equations for radial positions of surfaces S_1 and S_2 are given respectively by

$$r_{1o} = \frac{t_o - e}{\sin\alpha}, \quad r_{1f} = \frac{t_f - e}{\sin\alpha} \tag{2}$$

where e is the distance of origin O_1 from the axis of symmetry and $t_o=t_{1o}+t_{2o}$ and $t_f=t_{1f}+t_{2f}$. Minimization of the total power determines the value of parameter e. From Fig. 1, it can be seen that when $e=0$, origin O_1 coincides with O_2 and both layers deform to the same reduction. When $e=t_{2o}$, the inner layer remains un-deformed while the outer layer deforms to cover the inner layer and for $0<e<t_{2o}$, the layers deform to different reductions.

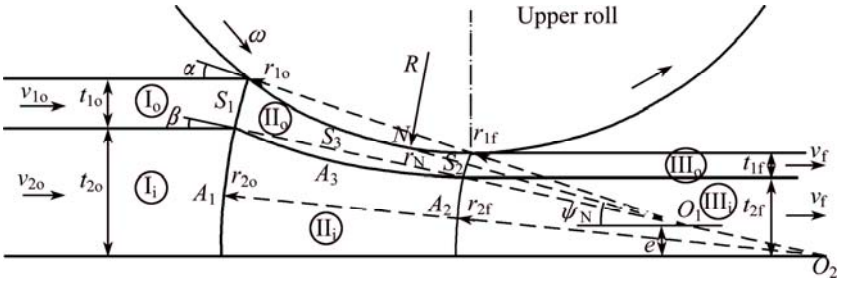

Fig. 1 Schematic diagram of rolling of non-bonded sandwich sheets and deformation regions

Angle α is the angle of the line connecting the initial point of the contact arc to the final point of the contact arc with axis of symmetry. The equation, which relates the processing parameters to the angle α is

$$\alpha = \arctan^{-1}\left[\frac{t_o - t_f}{\sqrt{(t_o - t_f)(2R + t_f - t_o)}}\right] \tag{3}$$

The center of cylindrical surfaces A_1 and A_2 is O_2 and they are located at distances r_{2o} and r_{2f} from the origin O_2, respectively. The mathematical equations for radial positions of them are defined by

$$r_{2o} = \frac{t_{2o}}{\sin\beta},\ \ r_{2f} = \frac{t_{2f}}{\sin\beta} \tag{4}$$

where β, as shown in Fig. 1, is the angle of the line connecting the initial point of the interface surface to the final point of the interface with axis of symmetry and it is determined by

$$\sin\beta = \frac{t_{2o} - e}{t_o - e}\sin\alpha \tag{5}$$

The angular position of the arc of contact as a function of the radial distance from the origin O_1, $\psi(r)$, is given by solving the following equation:

$$(r\sin\psi - R - t_f + e)^2 + (r\cos\psi - \frac{t_f - e}{\tan\alpha})^2 = R^2 \tag{6}$$

3 Upper bound analysis

The accuracy of predictions based on the upper bound method strongly depends on the kinematically admissible velocity field chosen. In each individual region, the velocity field and its derivatives should be continuous. The velocity field that has been derived from incompressibility condition and satisfies the velocity boundary conditions is a kinematically admissible velocity field.

3.1 Velocity components in deformation regions

In region II_o, the velocity of outer layer can be given by assuming proportionality distances from the horizontal line which goes through origin O_1, as

$$\begin{cases} \dot{U}_r = -v_{1o}\dfrac{r_{1o}}{r}\dfrac{\sin\alpha}{\sin\psi}\cos\theta \\ \dot{U}_\theta = -v_{1o}\ r_{1o}\dfrac{\sin\alpha}{\sin\psi}\dfrac{\partial\psi}{\partial r}\cot\psi\sin\theta \\ \dot{U}_z = 0 \end{cases} \tag{7}$$

The method presented in this work is similar to the method proposed in Refs. [12,13] for constructing kinematically admissible velocity fields for plane strain problems to analyse the deformation of the material in extrusion process. It can be verified that the velocity field expressed in Eq. (7) is a kinematically admissible velocity field, which means that it satisfies all the velocity boundary conditions and volume constancy. From Fig. 1, it is known that the velocity field satisfies all the velocity boundary conditions.

Within deformation region II_i, the outer layer material acts as a curved die for deformation of the inner layer and the outer material flows as if it is flowing through a curved die having an equation $\psi_i(r)$, which is the angular position of the interface surface as a function of the radial distance from the origin O_2. The governing equations for the velocity field of the deformation zone II_i in the cylindrical coordinate system with origin O_2 are similar to those presented in Eq. (7). They are

$$\begin{cases} \dot{U}_r = -v_{2o}\dfrac{r_{2o}}{r}\dfrac{\sin\beta}{\sin\psi_i}\cos\theta \\ \dot{U}_\theta = -v_{2o}\ r_{2o}\dfrac{\sin\beta}{\sin\psi_i}\dfrac{\partial\psi_i}{\partial r}\cot\psi_i\sin\theta \\ \dot{U}_z = 0 \end{cases} \tag{8}$$

Based on the developed velocity fields for inner and outer layers, the strain rate field can be obtained by

$$\begin{cases} \dot{\varepsilon}_{rr} = \dfrac{\partial\dot{U}_r}{\partial r},\ \ \dot{\varepsilon}_{\theta\theta} = \dfrac{1}{r}\dfrac{\partial\dot{U}_\theta}{\partial\theta} + \dfrac{\dot{U}_r}{r},\ \ \dot{\varepsilon}_{zz} = \dfrac{\partial\dot{U}_z}{\partial z} \\ \dot{\varepsilon}_{r\theta} = \dfrac{1}{2}(\dfrac{\partial\dot{U}_\theta}{\partial r} + \dfrac{1}{r}\dfrac{\partial\dot{U}_r}{\partial\theta} - \dfrac{\dot{U}_\theta}{r}) \\ \dot{\varepsilon}_{\theta z} = \dfrac{1}{2}(\dfrac{\partial\dot{U}_\theta}{\partial z} + \dfrac{1}{r}\dfrac{\partial\dot{U}_z}{\partial\theta}) \\ \dot{\varepsilon}_{zr} = \dfrac{1}{2}(\dfrac{\partial\dot{U}_r}{\partial z} + \dfrac{\partial\dot{U}_z}{\partial r}) \end{cases} \tag{9}$$

For deformation region II_o,

$$\begin{cases} \dot{\varepsilon}_{rr} = -\dot{\varepsilon}_{\theta\theta} = v_{1o}\dfrac{r_{1o}}{r^2}\dfrac{\sin\alpha}{\sin\psi}(1 + r\dfrac{\partial\psi}{\partial r}\cot\psi)\cos\theta \\ \dot{\varepsilon}_{r\theta} = \dfrac{1}{2}v_{1o}\ \dfrac{r_{1o}}{r^2}\dfrac{\sin\alpha}{\sin\psi}[1 - r^2\cot\psi\dfrac{\partial^2\psi}{\partial r^2} + \\ \qquad r^2(1+\cot^2\psi)(\dfrac{\partial\psi}{\partial r})^2 + \\ \qquad \cot^2\psi(\dfrac{\partial\psi}{\partial r})^2 + r\cot\psi\dfrac{\partial\psi}{\partial r}]\sin\theta \\ \dot{\varepsilon}_{zz} = \dot{\varepsilon}_{\theta z} = \dot{\varepsilon}_{zr} = 0 \end{cases} \tag{10}$$

where $\partial\psi/\partial r$ can be obtained by differentiation of Eq. (6) as

$$\frac{\partial\psi}{\partial r} = \frac{r - (R + t_f - e)\sin\psi - \dfrac{t_f - e}{\tan\alpha}\cos\psi}{r[(R + t_f - e)\cos\psi - \dfrac{t_f - e}{\tan\alpha}\sin\psi]} \tag{11}$$

The strain rate field for deformation region $\mathrm{II_i}$,

$$\begin{cases}\dot{\varepsilon}_{rr}=-\dot{\varepsilon}_{\theta\theta}=v_{2\mathrm{o}}\dfrac{r_{2\mathrm{o}}}{r^2}\dfrac{\sin\beta}{\sin\psi_{\mathrm{i}}}(1+r\dfrac{\partial\psi_{\mathrm{i}}}{\partial r}\cot\psi_{\mathrm{i}})\cos\theta\\ \dot{\varepsilon}_{r\theta}=\dfrac{1}{2}v_{2\mathrm{o}}\dfrac{r_{2\mathrm{o}}}{r^2}\dfrac{\sin\beta}{\sin\psi_{\mathrm{i}}}[1-r^2\cot\psi_{\mathrm{i}}\dfrac{\partial^2\psi_{\mathrm{i}}}{\partial r^2}+\\ \quad r^2(1+\cot^2\psi_{\mathrm{i}})(\dfrac{\partial\psi_{\mathrm{i}}}{\partial r})^2+\\ \quad \cot^2\psi_{\mathrm{i}}(\dfrac{\partial\psi_{\mathrm{i}}}{\partial r})^2+r\cot\psi_{\mathrm{i}}\dfrac{\partial\psi_{\mathrm{i}}}{\partial r}]\sin\theta\\ \dot{\varepsilon}_{zz}=\dot{\varepsilon}_{\theta z}=\dot{\varepsilon}_{zr}=0\end{cases}\tag{12}$$

The velocity fields for the inner and the outer layers, during rolling of sandwich sheets, are used to estimate the various energy deformation rates. The total deforming power required for the process can be split up into three parts: 1) internal power of deformation for inner and outer layers sheets; 2) the power losses due to shear at surfaces of the velocity discontinuities; and 3) the power losses due to friction along the interface and contact surfaces.

3.2 Determination of power terms of outer layer

The internal power of regions $\mathrm{I_o}$ and $\mathrm{III_o}$ are zero and the equation to calculate the internal power of deformation in region $\mathrm{II_o}$ is

$$\dot{W}_{\mathrm{iII_o}}=\frac{2\sigma_{\mathrm{o}}}{\sqrt{3}}\int_{r_{\mathrm{1f}}}^{r_{\mathrm{1o}}}\int_{\psi_{\mathrm{1i}}(r)}^{\psi(r)}\sqrt{\dot{\varepsilon}_{rr}^2+\dot{\varepsilon}_{r\theta}^2}\ r\,\mathrm{d}\theta\,\mathrm{d}r\tag{13}$$

where $\sigma_{0\mathrm{o}}$ is the mean flow stress of outer layer and is determined by

$$\sigma_{0\mathrm{o}}=\frac{\int_0^{\bar{\varepsilon}}\bar{\sigma}_{\mathrm{o}}\,\mathrm{d}\bar{\varepsilon}}{\bar{\varepsilon}},\quad \bar{\varepsilon}=\frac{2}{\sqrt{3}}\ln\frac{t_{\mathrm{o1}}}{t_{\mathrm{f1}}}\tag{14}$$

where $\psi_{1\mathrm{i}}(r)$ is the angular position of the interface surface as a function of the radial distance from the origin O_1 and is given by

$$\psi_{1\mathrm{i}}(r)=\arcsin^{-1}\left[\frac{\sin\beta}{\sin\alpha}\sin\psi(r)\right]\tag{15}$$

The equation for the power loss along a shear surface is

$$\dot{W}_{\mathrm{S}}=\frac{\sigma_0}{\sqrt{3}}\int_S|\Delta v|\,\mathrm{d}S\tag{16}$$

where $|\Delta v|$ is the absolute value of the difference between the velocity components tangent to the boundary, S is the velocity discontinuity surface. The velocity discontinuity between the regions is determined using the velocity of the neighboring region and the direction of motion in each region as

$$|\Delta v_{1\mathrm{o}}|=v_{1\mathrm{o}}(1+r_{1\mathrm{o}}\frac{\partial\psi}{\partial r}\cot\alpha)\sin\theta\tag{17}$$

$$|\Delta v_{2\mathrm{o}}|=v_{1\mathrm{o}}(1+r_{1\mathrm{o}}\frac{t_{1\mathrm{f}}}{t_{1\mathrm{o}}}\frac{\partial\psi}{\partial r}\cot\alpha)\sin\theta\tag{18}$$

At the entrance and the exit discontinuity surfaces S_1 and S_2, by placing $(\psi=\alpha,\ r=r_{1\mathrm{o}})$ and $(\psi=\alpha,\ r=r_{1\mathrm{f}})$ into Eq. (11), it follows that

$$r_{1\mathrm{o}}\frac{\partial\psi}{\partial r}=\frac{2(t_{\mathrm{o}}-t_{\mathrm{f}})}{R\sin 2\alpha}-\tan\alpha\tag{19}$$

$$r_{1\mathrm{f}}\frac{\partial\psi}{\partial r}=-\tan\alpha\tag{20}$$

Then, the shear power losses along surfaces S_1 and S_2, respectively, become

$$\dot{W}_{S,S_1}=\frac{\sigma_{\mathrm{o}}}{\sqrt{3}}v_{1\mathrm{o}}\,r_{1\mathrm{o}}\frac{t_{\mathrm{o}}-t_{\mathrm{f}}}{R}\frac{\cos\beta-\cos\alpha}{\sin^2\alpha}\tag{21}$$

$$\dot{W}_{S,S_2}=0\tag{22}$$

The power dissipated over the contact surface between the rigid roll and the outer layer can be calculated using

$$\dot{W}_{\mathrm{f}}=\frac{\sigma_0}{\sqrt{3}}m_1\int_S|\Delta v|\,\mathrm{d}S\tag{23}$$

where the constant friction factor, m_1, is the friction factor between the upper layer and roll surface and it can take on values from 0 to 1.

The element of the surface of contact surface (per unit with of sheet) is

$$\mathrm{d}S=\sqrt{1+(r\frac{\partial\psi}{\partial r})^2}\,\mathrm{d}r\tag{24}$$

Since the velocity vector at a point on the contact surface is tangential to the roll surface and since the tangential velocity discontinuity is in the same direction with the tangent of the contact surface, the amount of velocity discontinuity can be expressed as follows:

$$|\Delta v|=|\dot{U}_r\cos\eta+\dot{U}_\theta\sin\eta+R\omega|\tag{25}$$

where ω is the angular velocity of the roll, $R\omega$ is the peripheral velocity of the roll and η is the local angle of the contact surface with respect to the local radial velocity component and

$$\cos\eta=\frac{1}{\sqrt{1+(r\frac{\partial\psi}{\partial r})^2}},\quad \sin\eta=\frac{r\frac{\partial\psi}{\partial r}}{\sqrt{1+(r\frac{\partial\psi}{\partial r})^2}}\tag{26}$$

Placing Eqs. (24)−(26) into Eq. (23), the frictional power loss per unit width of sheet along contact surface can be determined as

$$\dot{W}_{\mathrm{f},S_3}=\frac{\sigma_{\mathrm{o}}}{\sqrt{3}}m_1v_{1\mathrm{o}}r_{1\mathrm{o}}\int_{r_{1\mathrm{f}}}^{r_{1\mathrm{o}}}\left|\frac{1}{r}\frac{\sin\alpha}{\tan\psi}+r\frac{\sin\alpha}{\tan\psi}(\frac{\partial\psi}{\partial r})^2-\frac{R\omega}{v_{1\mathrm{o}}\ r_{1\mathrm{o}}}\sqrt{1+(r\frac{\partial\psi}{\partial r})^2}\right|\mathrm{d}r \tag{27}$$

3.3 Determination of power terms of inner layer

The internal powers of regions $\mathrm{I_i}$ and $\mathrm{III_i}$, are zero and the equation to calculate the internal power of deformation in region $\mathrm{II_i}$ is determined as

$$\dot{W}_{\mathrm{i,IIi}}=\frac{2\sigma_{\mathrm{i}}}{\sqrt{3}}\int_{r_{2\mathrm{f}}}^{r_{2\mathrm{o}}}\int_0^{\psi_{\mathrm{i}}(r)}\sqrt{\dot{\varepsilon}_{rr}^2+\dot{\varepsilon}_{r\theta}^2}\ r\,\mathrm{d}\theta\,\mathrm{d}r \tag{28}$$

where σ_{oi} is the mean flow stress of the inner layer material and is determined as

$$\sigma_{0\mathrm{i}}=\frac{\int_0^{\bar{\varepsilon}}\bar{\sigma}_{\mathrm{i}}\,\mathrm{d}\bar{\varepsilon}}{\bar{\varepsilon}},\quad \bar{\varepsilon}=\frac{2}{\sqrt{3}}\ln\frac{t_{2\mathrm{o}}}{t_{2\mathrm{f}}} \tag{29}$$

where $\psi_{\mathrm{i}}(r)$ is the angular position of the interface surface as a function of the radial distance from the origin O_2 and is given by

$$\tan\psi_{\mathrm{i}}=\frac{e+r_1\sin\psi_{1\mathrm{i}}}{r_1\cos\psi_{1\mathrm{i}}+\dfrac{e}{\tan\beta}} \tag{30}$$

And the radial distance r of the interface surface from origin O_2 is defined by

$$r=\sqrt{(e+r_1\sin\psi_{1\mathrm{i}})^2+(r_1\cos\psi_{1\mathrm{i}}+\frac{e}{\tan\beta})^2} \tag{31}$$

where r_1 is the radial distance of the radial position from the origin O_1.

The velocity discontinuity between the neighboring regions is

$$\left|\Delta v_{1\mathrm{i}}\right|=v_{2\mathrm{o}}\,(1+r_{2\mathrm{o}}\frac{\partial\psi_{\mathrm{i}}}{\partial r}\cot\alpha)\sin\theta \tag{32}$$

$$\left|\Delta v_{2\mathrm{i}}\right|=v_{2\mathrm{o}}\,(1+r_{2\mathrm{o}}\frac{t_{2\mathrm{f}}}{t_{2\mathrm{o}}}\frac{\partial\psi}{\partial r}\cot\alpha)\sin\theta \tag{33}$$

Substituting Eqs. (32) and (33) into Eq. (16), the shear power losses (per unit of width) along surfaces A_1 and A_2, respectively, become

$$\dot{W}_{S,A_{\mathrm{i}}}=\frac{\sigma_{\mathrm{i}}}{\sqrt{3}}v_{2\mathrm{o}}\,r_{2\mathrm{o}}\int_0^{\beta}(1+r_{2\mathrm{o}}\frac{\partial\psi_{\mathrm{i}}}{\partial r}\cot\alpha)\sin\theta\mathrm{d}\theta \tag{34}$$

$$\dot{W}_{S,A_2}=\frac{\sigma_{\mathrm{i}}}{\sqrt{3}}v_{2\mathrm{o}}\,r_{2\mathrm{o}}\int_0^{\beta}(1+r_{2\mathrm{o}}\frac{t_{2\mathrm{f}}}{t_{2\mathrm{o}}}\frac{\partial\psi}{\partial r}\cot\alpha)\sin\theta\mathrm{d}\theta \tag{35}$$

3.4 Power consumption due to relative motion between sheet layers

While the sandwich sheet is rolled into the deformation region, there is a relative sliding at the interface between regions $\mathrm{II_o}$ and $\mathrm{II_i}$ and the frictional power is consumed along the interface surface between the inner and outer layers due to the difference in velocities. The power consumption over interface per unit with of sheet may be expressed as

$$\dot{W}_{\mathrm{f},A_3}=\frac{\sigma_{\mathrm{i}}+\sigma_{\mathrm{o}}}{2\sqrt{3}}m_2\left|(\Delta v_{\mathrm{m}})_{\mathrm{i,o}}\right|l \tag{36}$$

where $\left|(\Delta v_{\mathrm{m}})_{\mathrm{i,o}}\right|$ is the absolute value of the difference of mean values of velocity of inner and outer layers over the interface, m_2 is the friction factor between the two layers and l is the length of the interface curve and is given by

$$l=\int_{r_{1\mathrm{f}}}^{r_{1\mathrm{o}}}\sqrt{1+(r\frac{\partial\psi_{1\mathrm{i}}}{\partial r})^2}\,\mathrm{d}r \tag{37}$$

The mean value of velocity of outer layer over the interface surface is

$$\left|(\Delta v)_{\mathrm{m}}\right|_{\mathrm{o}}=r_{1\mathrm{o}}v_{1\mathrm{o}}\frac{\int_{r_{1\mathrm{f}}}^{r_{1\mathrm{o}}}\left|\frac{1}{r}\frac{\sin\alpha}{\tan\psi_{1\mathrm{i}}}+r\frac{\sin\alpha}{\tan\psi_{1\mathrm{i}}}(\frac{\partial\psi_{1\mathrm{i}}}{\partial r})^2\right|\mathrm{d}r}{l} \tag{38}$$

Similarly, for inner layer, we have

$$\left|(\Delta v)_{\mathrm{m}}\right|_{\mathrm{i}}=r_{2\mathrm{o}}v_{2\mathrm{o}}\frac{\int_{r_{2\mathrm{f}}}^{r_{2\mathrm{o}}}\left|\frac{1}{r}\frac{\sin\alpha}{\tan\psi_{\mathrm{i}}}+r\frac{\sin\alpha}{\tan\psi_{\mathrm{i}}}(\frac{\partial\psi_{\mathrm{i}}}{\partial r})^2\right|\mathrm{d}r}{l} \tag{39}$$

The resultant tangential mean velocity discontinuity at the interface surface between the inner and the outer layers, may be expressed as

$$\left|(\Delta v_{\mathrm{m}})_{\mathrm{i,o}}\right|=\left|(\Delta v_{\mathrm{m}})_{\mathrm{i}}-(\Delta v_{\mathrm{m}})_{\mathrm{o}}\right| \tag{40}$$

Substituting for l and $(\Delta v_{\mathrm{m}})_{\mathrm{i,o}}$ from Eqs. (37) and (40), respectively into Eq. (36), the frictional power loss per unit width, over interface surface A_3 can be determined.

4 Position of neutral point

In the neutral point, the peripheral velocity of roll is equal to the material velocity. Hence, the relative velocity between the outer layer and the roll is zero at the neutral point, point N in Fig. 1 with radial and angular positions r_N and ψ_N, respectively. On the left hand of the point N, the roll surface moves faster than the sheet material, whereas on the right hand of the point N, material moves faster than the roll surface. The velocity vector at a point on the roll surface is coinciding with the tangential line passing through that point. Since the velocity discontinuity is in the same direction with the tangent of the roll surface, their values are the same in neutral point N, then

$$\dot{U}_r\cos\eta+\dot{U}_\theta\sin\eta=-R\omega \tag{41}$$

Placing coordinates of the neutral point N ($r=r_N$, $\theta=\psi_N$) into Eq. (7), the values of the velocity components of the neutral point N can be determined. Substituting the velocity components of the neutral point N into the above equation and simplification, it follows that

$$v_{1o}\frac{r_{1o}}{r_N}\frac{\sin\alpha}{\tan\psi_N}+v_{1o}\,r_{1o}\,r_N\frac{\sin\alpha}{\tan\psi_N}(\frac{\partial\psi}{\partial r})^2=R\omega\sqrt{1+(r\frac{\partial\psi}{\partial r})^2} \tag{42}$$

5 Rolling torque, rolling force and contact pressure

By the upper bound model, the externally supplied power is less than or equal to the sum of the powers described in the previous sections. If one assumes the equality, then the total power is

$$J^*=\dot{W}_{i,II_o}+\dot{W}_{i,II_i}+\dot{W}_{S,S_1}+\dot{W}_{S,A_1}+\dot{W}_{S,A_2}+\dot{W}_{f,A_3}+\dot{W}_{f,S_3} \tag{43}$$

The total upper bound solution for rolling torque is given by

$$T=\frac{J^*}{\omega} \tag{44}$$

where T is the required rolling torque per unit width of the sheet.

Neglecting the contribution of the horizontal forces, the roll separating force per unit of width is calculated by the following equation [3]

$$F=\frac{J^*}{L\omega} \tag{45}$$

where F, J^*, L and ω are the rolling force per unit width of sheet, the rolling power calculated by the upper bound solution, the projected contact length and the angular velocity of roll, respectively. The contact length L is calculated as

$$L=\sqrt{2Rt_oh},\ h=1-\frac{t_f}{t_o} \tag{46}$$

where h is the reduction in total thickness.

The mean contact pressure at the interface between sheets may be expressed as

$$P_m=\frac{F}{L_i} \tag{47}$$

where L_i is the projected length of the interface between the outer and inner layers at the deformation region and with referring to Fig. 1, it is determined by

$$L_i=(r_{2o}-r_{2f})\cos\beta \tag{48}$$

Equation (43) reveals that the torque required for rolling of a symmetrical sandwich sheet becomes a function of the process parameters (thicknesses of initial and final sheet, friction factor, roll radius and roll angular velocity, etc.) and the two independent parameters, quantity r_N which determines the radial position of the neutral point and value of e. Therefore, minimization of Eq. (44) with respect to two independent parameters e and r_N will yield a lower upper bound solution for the rolling torque. In the present investigation, the integrals that are present in the power terms are evaluated by numerical integration. A computer program was used to perform the minimization process.

6 Results and discussion

A MATLAB program has been implemented for the previously derived equations and the rolling torque is calculated for a set of rolling conditions and a field giving the lowest torque is found. In this calculation, minimization of the total rolling power determines the values of two independent parameters e and r_N where e is limited between 0 and t_{2o}.

In order to verify the validity of the upper bound approach for rolling process of sandwich sheets presented in the present research, the results obtained from the theoretical model are compared with the available experimental data in Ref. [4]. The radii of the rolls are both 100 mm. The peripheral speeds of the rolls are both 5 m/min. Aluminum and mild steel sheets are employed as specimens. The flow stresses for mild steel and aluminum at room temperature are obtained as [6]

$\bar{\sigma}=193.8\,(\bar{\varepsilon})^{0.046}$ MPa for aluminum (Al) sheet with thickness of 1 mm;

$\bar{\sigma}=183.2\,(\bar{\varepsilon})^{0.045}$ MPa for aluminum (Al) sheet with thickness of 1.4 mm;

$\bar{\sigma}=944.8(\bar{\varepsilon})^{0.14}$ MPa for mild steel (SPCC)

Two combinations of sandwich sheets Al/SPCC/Al were tested. Figure 2 shows the comparisons of rolling force between the theoretical predictions and the experimental values for the first case. In this case, the initial total thickness of sandwich sheet is 3.8 mm. The rolling conditions and the combination of raw sheet are shown in Fig. 2. It is noted that the inner layer material is harder than the outer material. In the computation, the friction factors m_1 and m_2 which represent the friction factor between the roll and sheet and that between sheets, respectively, are taken to be 0.8 and 1.0, which are generally close to the conditions for dry friction. From this figure, the theoretical predictions coincide with the experimental data.

Figure 2 also shows that an increase in the reduction tends to increase the rolling force.

Figure 3 illustrates the comparison of the rolling

force between the theoretical predictions and the experimental measurements for the second case. In the second case, the total thickness is 3 mm and the rolling conditions of initial sandwich sheet are shown in the figure. Very high agreement between the predicted rolling forces and the experimental values is found. From Figs. 2 and 3, it is known that the rolling force increases with increasing the initial thickness ratio of the inner layer to the total thickness, because the inner layer material SPCC is harder than the outer layer material Al.

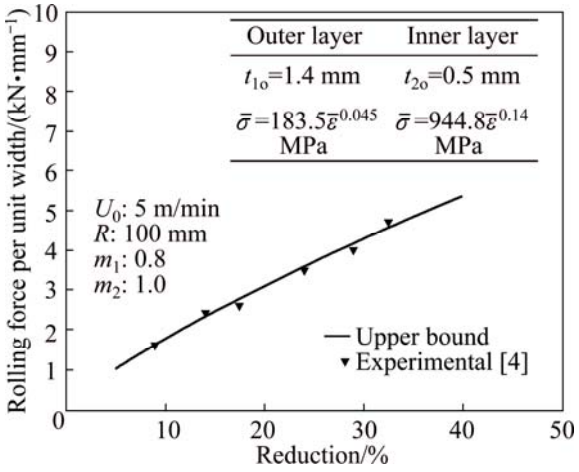

Fig. 2 Comparison of calculated rolling forces per unit of width with experimental data for different total thickness reductions for first case

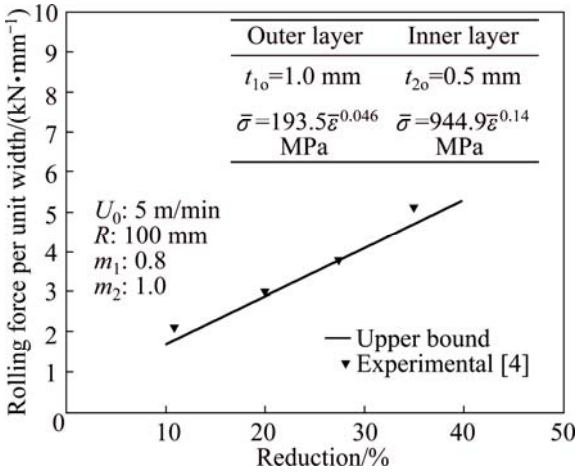

Fig. 3 Comparison of calculated rolling forces per unit of width with experimental data under different total thickness reduction for second case

For further validating the proposed deformation model, for rolling process of sandwich sheets, the results obtained from the theoretical analysis are also compared with the experimental data of Ref. [6]. In the computation, the friction factors m_1 and m_2 are taken to be 0.7 and 0.9, respectively.

Figure 4 illustrates the comparisons of the rolling force between theoretical predictions and experimental measurements. Figure 4 clearly reveals that the predictions show good agreement with the experimental results. Figure 5 illustrates the comparisons of the rolling force between the theoretical predictions and the experimental measurements. The results show a good agreement between the upper bound data and the experimental values. It can be seen that the mean contact pressure is increased by increasing the reduction in thickness.

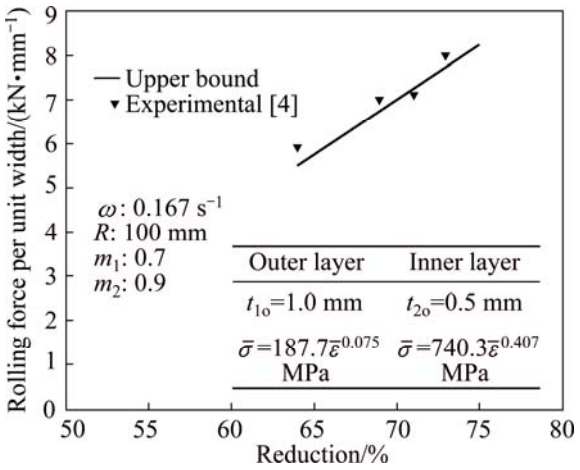

Fig. 4 Comparison of analytical roll force per unit of width with experimental values

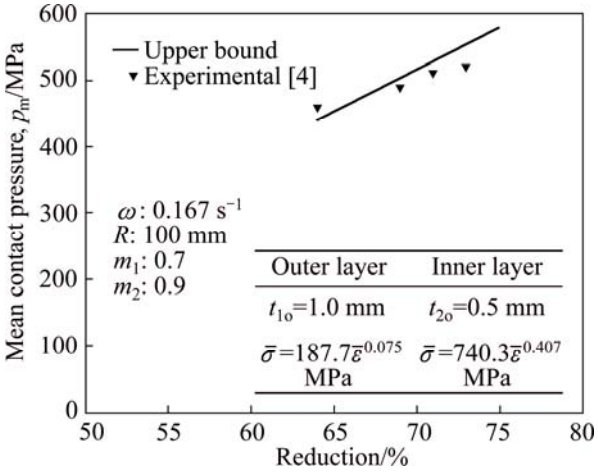

Fig. 5 Comparison of calculated mean contact pressure per unit of width with experimental values

It is observed that the proposed velocity field leads to a computationally efficient procedure which gives good agreement with the experimental data. From the comparison, it is clear that the proposed velocity field employed in the model of sandwich sheet rolling is valid for simulating the general rolling of initially non-bonded sandwich sheets.

The calculations have been carried out under various rolling conditions and the effects of the reduction,

friction factors, ratio of roll radius to total sheet thickness, etc., are considered in the analysis. The roll radius R and the flow stress of the outer layer σ_{0o} are fixed. The radii of the rolls are both 100 mm. The peripheral speeds of the rolls are both 40 mm/s.

The effect of the total thickness of sandwich sheet upon the rolling force is plotted in Fig. 6.

The rolling conditions employed are shown in the figure. As it is expected, for a given value of the thickness reduction, the rolling force increases with increasing the total thickness of the sandwich sheet. From this figure, it is seen that an increase in the thickness reduction tends to increase the rolling force.

The relation between the values of the final thickness of each layer can also be assessed. Figure 7 shows the effects of the thickness reduction upon the thickness ratio of the outer layer at the exit, t_{1f}/t_f. From Fig. 7, we know that the final thickness ratios of outer layer are always less than that at the entrance, t_{1o}/t_o, which is 0.4. This is reasonable because the outer layer is softer than the inner layer. It is also found that t_{1f}/t_f decreases with increasing reduction, which means that the greater the reduction is, the more non-uniform the plastic deformation of sheets becomes. Accordingly, the difference between t_{1f}/t_f and t_{1o}/t_o increases as the reduction increases.

Figure 8 illustrates the effects of the friction factor between the roll and the sheet on the total rolling power. Apparently, the total rolling power increases with increasing reduction and friction factor, m_1. From Fig. 8, it can be seen that the difference between rolling power curves increases as the reduction increases.

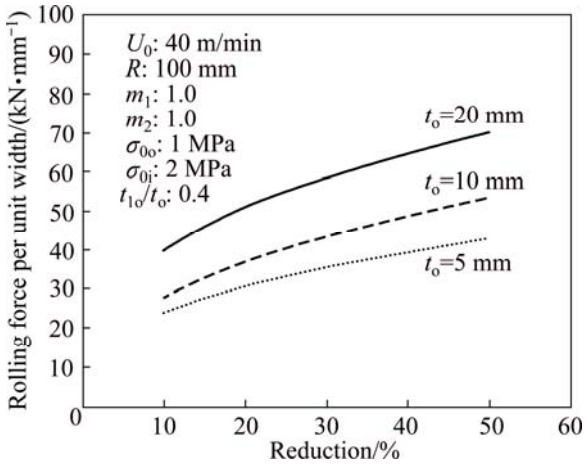

Fig. 6 Effect of initial total thickness on rolling force per unit of width

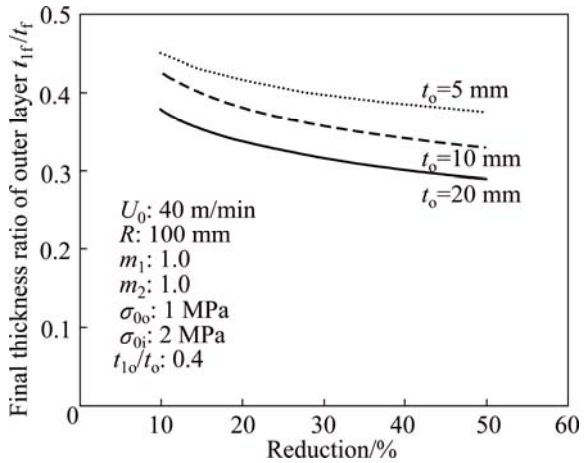

Fig. 7 Effect of total thickness upon final thickness ratio of outer layer

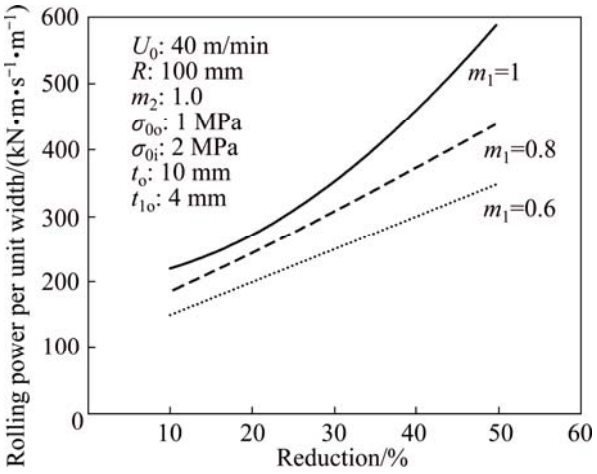

Fig. 8 Effect of friction factor m_1 on rolling power per unit of width as function of thickness reduction

The effect of the friction factor between inner and outer layer m_2 on the rolling torque is also examined and it is shown in Fig. 9. It is clear that the rolling torque increases with the friction at the interface and reduction.

The effects of the reduction and the roll radius, R, upon the rolling torque are indicated in Fig. 10. As it is expected, apparently, the rolling torque increases with increasing reduction for R=50, 200 or 300 mm, whereas T increases little with increasing reduction for R=100 or 75 mm.

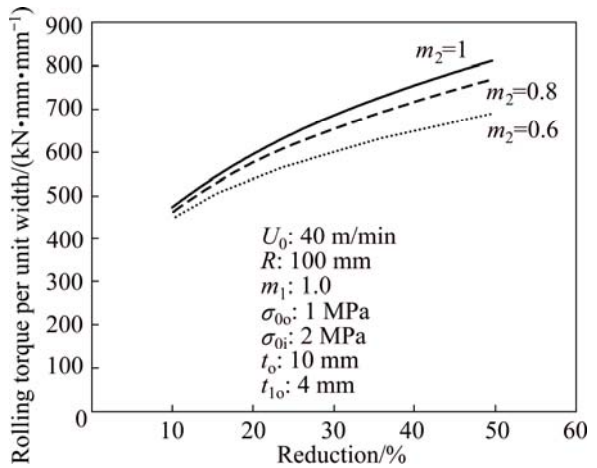

Fig. 9 Effect of friction factor m_2 between layers on roll torque as function of thickness reduction

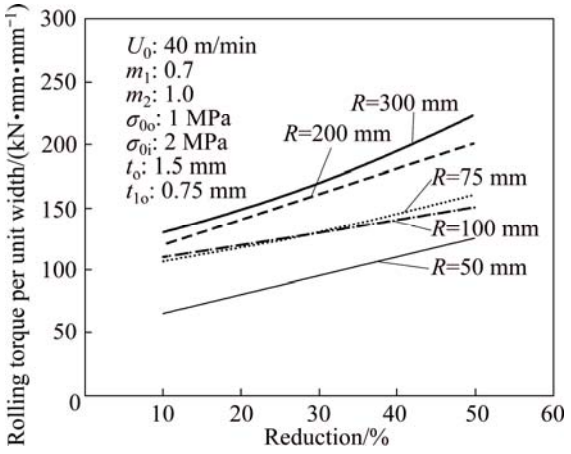

Fig. 10 Effect of roll radius upon roll torque per unit of width as function of thickness reduction

7 Conclusions

1) An admissible velocity field for use in upper bound analysis of rolling process was developed.

2) Equations for the strain rate field, power dissipation within the plastic region, at the velocity discontinuities and at the friction surface, have been developed in terms of ordinary integrals. These allow the calculation of the total power required for the rolling process.

3) The theoretical predictions of rolling torque are found to be in very good agreement with those obtained experimentally.

References

[1] MAKI S, NAKAMURA M, MATSUDA T, NAGAI N. Influence of rolling condition on bond strength in cladding of steel sheet with aluminum [J]. Journal of Japan Society for Technology of Plasticity, 1989, 30: 71.

[2] SHIROTA T, DENDO T. Effect of rolling conditions on bonding behavior in cold clad rolling by planetary mill [J]. Journal of Japan Society for Technology of Plasticity, 1983, 24: 480.

[3] HWANG Y M, HSU H H, LEE H J. Analysis of sandwich sheet rolling by stream function method [J]. International Journal of Mechanical Sciences, 1995, 37: 297−315.

[4] HWANG Y M, CHEN T H, HSU H S. Analysis of asymmetrical clad sheet rolling by stream function method [J]. International Journal of Mechanical Sciences, 1996, 38: 443−460.

[5] HWANG Y M, HSU H H, LEE H J. Analysis of plastic instability during sandwich sheet rolling [J]. International Journal of Machine Tools Manufacture, 1996, 36: 47−62.

[6] HWANG Y M, HSU H H, HWANG Y L. Analytical and experimental study on bonding behavior at the roll gap during complex rolling of sandwich sheets [J]. International Journal of Mechanical Sciences, 2000, 42: 2417−2437.

[7] MALEKI H, BAGHERZADEH S, MOLLAAEI-DARIANI B, ABRINIA K. Analysis of bonding behavior and critical reduction of two-layer strips in clad cold rolling process [J]. Journal of Materials Engineering and Performance, 2013, 22: 917−925.

[8] ZHANG S, SONG B, WANG X, ZHAO D. Analysis of plate rolling by MY criterion and global weighted velocity field [J]. Applied Mathematical Modelling, 2014, 38: 3485−3494.

[9] MARTINS P A F. Manuel barata marques MJ upper bound analysis of plane strain rolling using a flow function and the weighted residuals method [J]. Int J Numer Meth Eng, 1999, 44: 1671−1683.

[10] DOGRUOGLU A N. On constructing kinematically admissible velocity fields in cold sheet rolling [J]. J Mater Process Technol, 2001, 110: 287−299.

[11] MOON C H, LEE Y. Approximate model for predicting roll force and torque in plate rolling which peening effect considered [J]. ISIJ Int, 2008, 48: 1409−1418.

[12] HAGHIGHAT H, AMJADIAN P. A generalized velocity field for plane strain extrusion through arbitrarily curved dies [J]. ASME Journal of Manufacturing Science and Engineering, 2011, 133: 041006.

[13] HAGHIGHAT H, SHAYESTEH H. Upper bound analysis for hybrid sheet metals extrusion process through curved dies [J]. Transactions of Nonferrous Metals Society of China, 2014, 24: 3285−3292.

非粘接夹层板轧制过程的上界分析

Heshmatollah HAGHIGHAT, Pedram SAADATI

Mechanical Engineering Department, Razi University, Kermanshah, Iran

摘　要：利用上界方法研究非粘接夹层板的轧制过程。提出了一个变形模型，建立各速率分量间的数学关系。将获得的内功。剪切功和摩擦功的表达式应用到上界模型中。通过分析，得到了轧制力、平均接触压强和各层的最终厚度。通过对比理论预测结果和文献中的实验数据，讨论了分析模型的有效性。分析了不同轧制条件(流变应力比，原料板材初始厚度比，总压下量)对轧制力矩的影响。建立的分析模型具有高的准确性。

关键词：平面轧制；夹层板；上界方法

(Edited by Yun-bin HE)